Nonlinear Control of Single-Phase PWM Rectifiers with Inherent Current-Limiting Capability

George C. Konstantopoulos, *Member, IEEE,* and Qing-Chang Zhong, *Senior Member, IEEE*

Abstract—**In this paper, a nonlinear controller with a current-limiting property is proposed to guarantee accurate dc output voltage regulation and unity power factor operation for single-phase PWM rectifiers without the need of a phase-locked-loop (PLL). The proposed current-limiting controller is fully independent of the system parameters and can guarantee asymptotic stability and convergence to a unique solution for the closed-loop system using nonlinear control theory. Without requiring the instantaneous measurement of the grid voltage, a PLL, an external limiter or a saturation unit, the proposed strategy guarantees that the input current of the rectifier will always remain below a given value. An analytic framework for selecting the controller parameters is also presented to provide a complete controller design procedure and it is also proven that the current-limiting property is maintained even when the grid voltage drops. Extensive experimental results are presented to verify the proposed controller when the load changes, the reference dc output voltage changes and the grid voltage drops.**

Index Terms—**PWM rectifiers, nonlinear control, current limit, asymptotic stability, grid voltage dip**

I. Introduction

AC/DC power converters are widely used in power systems to integrate loads or power sources to the electric grid by operating as a rectifier or an inverter, respectively [1], [2], [3], [4]. Depending on the application, ac/dc converters can be single-phase or three-phase with main tasks the accurate dc bus voltage regulation and power factor correction (PFC). For rectifiers, the PFC can be achieved by controlling the input current to be in phase with the input voltage and has been extensively studied in the literature [5], [6], [7], [8], [9], [10], [11], [12].

AC/DC converters are inherently nonlinear systems due to their switching operating function. Among these devices, the single-phase full-bridge or H-bridge rectifier represents a common PFC converter operating in pulse-width-modulating (PWM) mode and its model can be generalized in the three-phase converter case [9], [13], [14], [15], [16]. Therefore, several researchers have developed control strategies for single-phase rectifiers to achieve both dc output voltage regulation and unity power factor operation. The most commonly used method includes a cascaded structure where an outer loop is used to control the dc output voltage and an inner current loop is used to control the input current to be in phase with the input voltage. In the traditional control methods, a Proportional-Integral (PI) controller is included into the outer loop and the inner current controller usually consists of a hysteresis current method [5], [17], [18], [19]. Additionally, the cascaded control structure can be combined with intelligent techniques such as fuzzy control to incorporate a sensorless design, as described in [20]. The traditional control methods have a simple structure and are effective in practice but they lack from a rigorous stability theory for the complete closed-loop system. Although for rectifier applications, boost-type PFC rectifier can be used instead of full-bridge rectifiers [21], the efficiency of these converters is significantly reduced and they result in higher power losses, especially for high-power applications [22].

Due to the nonlinear dynamic model of the converter, which can be obtained using the average analysis [23], [24], passivity-based control represents a powerful tool and can be effectively applied to achieve both control tasks and guarantee global asymptotic stability of the closed-loop system [7], [12], [15]. Since the accurate knowledge of the load is required in this case, adaptive passivity-based structures have been developed to cope with the load uncertainty [25], [26], [12]. However, the control scheme still depends on the rest of the system parameters, i.e. the inductor, the capacitor and the measurement of the grid voltage. These parameters might not be accurately known a priori or might change during the system operation. Furthermore, more complicated loads can be connected at the rectifier output, (e.g. nonlinear, power converter-fed loads), which will increase the complexity of the model and consequently the controller design.

Furthermore, in practice, except from the requirement of an asymptotically stable closed-loop system solution, the input current should be maintained below a maximum value at all times for protection purposes. Hence, the development of current-limited rectifiers has been an active area of research for several decades [27], [28], [29], [30], [31]. Current limitation should be maintained at all times, especially during transients, load changes and input voltage sags, since these cases can be catastrophic for the rectifier as mentioned in [32], [33]. Although current limitation can be achieved with the advanced passivity-based methods under accurate knowledge of the system parameters, the traditional control techniques that are parameter-free require external current limiters, protection circuits or saturation units in the control design to limit the input current [34], [35], [36], [37], [38]. Several approaches

G. C. Konstantopoulos is with the Department of Automatic Control and Systems Engineering, The University of Sheffield, Sheffield, S1 3JD, UK, tel: +44-114 22 25637, fax: +44-114 22 25683 (e-mail: g.konstantopoulos@sheffield.ac.uk).

Q.-C. Zhong is with the Department of Electrical and Computer Engineering, Illinois Institute of Technology, Chicago, IL 60616, USA, and also with the Department of Automatic Control and Systems Engineering, The University of Sheffield, Sheffield, S1 3JD, UK (e-mail: zhongqc@ieee.org).

The financial support from the EPSRC, UK under Grant No. EP/J01558X/1 is greatly appreciated.

Some preliminary results were presented at the 2015 American Control Conference, Chicago, IL, 1-3 July 2015.

Corresponding author: Dr G. C. Konstantopoulos

also inherit a switching behavior between the normal operation and the current-limiting operation when the grid voltage drops [36], [39]. However, the use of saturation units can lead to undesired oscillations in several applications and asymptotic stability cannot be guaranteed, mainly due to integrator windup [32], [38]. Although anti-windup techniques can be inserted into the control design, traditional anti-windup methods lack from a rigorous stability analysis and modern anti-windup methods require the knowledge of the plant to guarantee stability [40], [41], [42]. Hence, it is a challenge to design a parameter-free controller with a simple and unified structure (no switching between control algorithms) that guarantees nonlinear stability of the closed-loop system and a given limit for the input current even under grid voltage sags.

In this paper, the single-phase full-bridge rectifier is investigated and a nonlinear controller that achieves accurate dc output voltage regulation, unity power factor operation and closed-loop stability with a limited input current, is developed. The proposed current-limiting nonlinear controller is fully independent of the system parameters, has a simple structure that leads to an easy implementation and achieves PFC at the input of the rectifier, which practically corresponds to PFC for the complete system. Using nonlinear Lyapunov theory, the controller operation is investigated and based on the input-to-state stability theory [43], closed-loop system stability in the sense of boundedness and eventually asymptotic convergence to a desired solution are proven. Particularly, for a given maximum RMS value I_{max} of the input current, the controller parameters can be suitably selected to guarantee that the input current will always remain bounded below this given value. This imposes a significant advantage compared to the existing parameter-free control techniques, since the current-limiting function is embedded into the original control structure, no external limiters or switching operation are required, leading to a continuous-time controller with the same dynamics that allows the investigation of stability. Moreover, only an initial estimation of the RMS value of the grid voltage (which is known in practice) is required, while the instantaneous measurement of the grid voltage or an additional PLL are not needed, thus further simplifying the controller implementation. The current-limiting capability is guaranteed even in the cases where the input voltage varies or rapidly drops, extending the proposed controller performance to both normal and abnormal operations of the grid, i.e. during grid faults. Extensive experimental results are provided for the single-phase full-bridge rectifier to illustrate the proposed approach and verify its current-limiting capability under load changes, reference dc output voltage changes and input voltage sags.

The paper is organized as follows: In Section II, the dynamic model of the rectifier is obtained and the main problem addressed in this paper is formulated. In Section III, the current-limiting controller is proposed and analyzed. Closed-loop system stability is proven, an analytic framework for selecting the controller parameters is presented and the controller performance is extended to the cases of input voltage variations. In Section IV, experimental results are provided to verify the proposed controller performance and finally, in Section V, some conclusions are drawn.

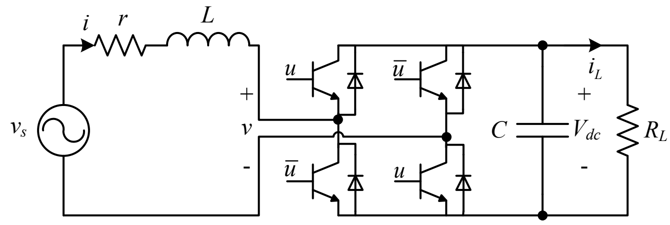

Figure 1. Single-phase full-bridge rectifier

II. Problem formulation

Consider a single-phase full-bridge rectifier feeding a resistive load as shown in Fig. 1. The converter consists of a boosting filter inductor L with a small parasitic resistance r, a dc capacitor C and 4 switches, whose switching signals are obtained from a PWM circuit taking values in the finite set $\{-1, 1\}$. Although the filter can be of different types (e.g. LCL) to achieve better harmonic attenuation for the grid current, here an L filter is considered for simplicity, since as it is explained below, at this stage, the current-limiting property and the stability are the main goals in this paper and not the power quality improvement. Parameter R_L represents the load resistance, i is the inductor current, V_{dc} is the dc output voltage, v is the converter input voltage and v_s is the single-phase grid voltage of the form $v_s = \sqrt{2}V_s \sin\omega t$, where V_s is the RMS grid voltage and ω is the grid angular frequency.

Using average model analysis [44], the nonlinear dynamic model of the system can be obtained using the Kirchhoff laws and the power equivalence of the converter as:

$$L\frac{di}{dt} = -ri - uV_{dc} + v_s \tag{1}$$

$$C\frac{dV_{dc}}{dt} = ui - \frac{V_{dc}}{R_L}, \tag{2}$$

where the control input $u = \frac{v}{V_{dc}}$ represents the continuous-time duty-ratio signal of the rectifier bounded in the range $[-1, 1]$, which is fed to the PWM generator to result in the discrete signals of the switching elements, while the grid voltage v_s represents an external uncontrolled input.

For system (1)-(2), the main tasks are to achieve accurate dc output voltage regulation and unity power factor operation. The average value of the dc output voltage $\bar{V}_{dc}$ should be always regulated at a given reference value V_{dc}^{ref}. The value of $\bar{V}_{dc}$ can be obtained from V_{dc} with a low-pass filter which rejects the second-order harmonics. In practice, the average value of the dc output voltage is calculated using a low-pass filter for V_{dc}^2 and then taking the square root of the result [45]. For the unity power factor operation, the current i should be in phase with the grid voltage v_s. In many applications of ac/dc converters (in the rectifier or inverter mode), power factor is also considered at the input of the converter [1], i.e., the current i to be in phase with the converter voltage v, since in most cases the filter inductor does not cause a significant phase shifting between the two voltages v_s and v.

Opposed to the traditional control methods [5], [17], [18] which lack from a rigorous nonlinear stability analysis and the advanced nonlinear controllers [7], [12], [15], [25], [26] that depend on the system parameters and the load dynamics, in this paper, the existence of a control structure for rectifiers is investigated that achieves both tasks and incorporates all of the following properties:

1) Complete independence from the system and load parameters;
2) Nonlinear closed-loop system stability with a given current limit;
3) Simple structure, based on the dynamics and the sensors required for the implementation.

III. Proposed controller design and stability analysis

A. Current-limiting nonlinear controller

Taking into account all of the controller properties mentioned in the previous section, the following current-limiting nonlinear controller is proposed:

$$u(t) = \frac{v(t)}{V_{dc}(t)} = \frac{w(t)i(t)}{V_{dc}(t)}, \tag{3}$$

where w represents a virtual resistance which changes according to the nonlinear dynamic equations

$$\dot{w} = c\left(\bar{V}_{dc} - V_{dc}^{ref}\right) w_q^2 \tag{4}$$

$$\dot{w}_q = -\frac{c(w-w_m)w_q}{\Delta w_{max}^2}\left(\bar{V}_{dc}-V_{dc}^{ref}\right) - k\left(\frac{(w-w_m)^2}{\Delta w_{max}^2}+w_q^2-1\right)w_q, \tag{5}$$

with c, k, w_m, Δw_{max} being positive constants. Note that for the implementation of (3), the current i should be the average value (sinusoidal) of the actual inductor current and can be obtained using a low-pass filter that rejects the higher harmonics (switching ripples), while V_{dc} represents the actual output voltage which includes the second-order harmonics.

From the controller structure, it becomes clear that the proposed controller is fully independent of the system parameters and does not require the instantaneous measurement of the grid voltage v_s or a PLL. When the average dc output voltage $\bar{V}_{dc}$ is regulated at the reference value V_{dc}^{ref}, then the controller parameter w is regulated at a constant value w^e, since $\dot{w} = 0$ from (4), and consequently (3) becomes

$$v(t) = w^e \cdot i(t) \tag{6}$$

which shows that the input voltage of the converter v is in phase with the current i and therefore unity power factor is achieved. As a result, both control tasks of the converter can be accomplished. In order to investigate whether this operation is possible, the controller dynamics are further analyzed.

For system (4)-(5), consider the Lyapunov function

$$W = \frac{(w-w_m)^2}{\Delta w_m^2} + w_q^2. \tag{7}$$

Its time derivative becomes

$$\dot{W} = -2k\left(\frac{(w-w_m)^2}{\Delta w_m^2} + w_q^2 - 1\right) w_q^2. \tag{8}$$

Therefore, if the initial conditions are chosen $w_0 = w_m$ and $w_{q0} = 1$, then $\dot{W}(t) = 0 \Rightarrow W(t) = W(0) = 1, \forall t \geq 0$ implying that w and w_q start and stay thereafter on the ellipse W_0:

$$W_0 = \left\{ w, w_q \in R : \frac{(w-w_m)^2}{\Delta w_m^2} + w_q^2 = 1 \right\}, \tag{9}$$

as shown in Fig. 2, which means that $w \in [w_{min}, w_{max}] = [w_m - \Delta w_m, w_m + \Delta w_m]$. Note that the same operation is obtained for any initial conditions w_0 and w_{q0} defined on the ellipse W_0, i.e. satisfying

$$\frac{(w_0-w_m)^2}{\Delta w_m^2} + w_{q0}^2 = 1, \tag{10}$$

with $w_{q0} > 0$. Hence, one can chose accordingly the parameters w_m and Δw_m in order for $w_{min} > 0$ at all times, i.e., it should be

$$w_m > \Delta w_m > 0, \tag{11}$$

which leads to $w(t) > 0, \forall t \geq 0$ and makes sense since it represents a virtual resistance in a rectifier application. The given bounds for the state w are important for limiting the current under a given maximum value as it will be analytically explained in the stability analysis described in Subsection III-B.

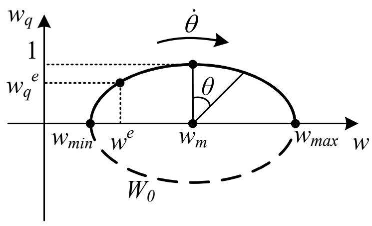

Figure 2. Controller states operation on ellipse W_0

When the controller states operate on the ellipse W_0, the controller dynamics (4)-(5) become

$$\dot{w} = c\left(\bar{V}_{dc} - V_{dc}^{ref}\right) w_q^2 \tag{12}$$

$$\dot{w}_q = -\frac{c(w-w_m)w_q}{\Delta w_{max}^2}\left(\bar{V}_{dc} - V_{dc}^{ref}\right). \tag{13}$$

For system (12)-(13), consider the following transformation

$$w - w_m = \Delta w_m \sin\theta \tag{14}$$

$$w_q = \cos\theta \tag{15}$$

which results after some simple calculations that

$$\dot{\theta} = \frac{c w_q \left(\bar{V}_{dc} - V_{dc}^{ref}\right)}{\Delta w_m}. \tag{16}$$

Expression (16) shows that the controller states w and w_q will move on the ellipse W_0 with angular velocity given by (16). Therefore, if $\bar{V}_{dc} \to V_{dc}^{ref}$, then $\dot{\theta} \to 0$ and both controller states will stop moving and converge to their steady-state values w^e and w_q^e respectively, as shown in Fig. 2. This makes possible the convergence of the complete converter system, since if w and w_q pass the desired equilibrium point during the transient response, the angular velocity will change sign and the states will oscillate around the equilibrium point.

Additionally, the controller states will move exclusively on the upper semi-ellipse of W_0 (Fig. 2), for initial conditions w_0 and $w_{q0} > 0$ that satisfy (10). The reason is that if w and w_q try to reach the horizontal axis, then $w_q \to 0$ and as a result from (16), $\dot{\theta} \to 0$ which forces the controller states to slow down independently from the difference $\bar{V}_{dc} - V_{dc}^{ref}$. This fact prohibits the existence of an oscillating behavior (limit cycle) for the controller dynamics themselves, i.e., they will never continuously travel around the ellipse W_0. In addition, since $w_q \to 0$ results in $\dot{w} \to 0$ in (4), this means that the integration slows down near the limits, i.e. when $w \to w_{min}$ or $w \to w_{max}$, and hence the proposed controller does not suffer from integrator windup issues. It should be mentioned that instead of the control dynamics (4)-(5) one can implement the proposed controller using (14), (15) and (16), and result in the same behavior since the two representations are equivalent.

B. Closed-loop system stability

From the previous analysis, it is clear that the proposed controller is able to achieve both precise output voltage regulation and unity power factor. However, in order to accomplish both tasks, closed-loop system stability should be guaranteed at all times. Since $w_m > \Delta w_m > 0$ and w_0, w_{q0} satisfy (10), then w and w_q are bounded with $w \in [w_{min}, w_{max}]$, where $w_{min} > 0$. By substituting (3) into the original system (1)-(2), it yields

$$L\frac{di}{dt} = -(r+w)\,i + v_s \tag{17}$$

$$C\frac{dV_{dc}}{dt} = \frac{wi^2}{V_{dc}} - \frac{V_{dc}}{R_L} \tag{18}$$

which is still a nonlinear system but (17) can be investigated as a time-varying system with $w \in [w_{min}, w_{max}]$, where w_{min}, $w_{max} > 0$.

Now, for system (17), consider the Lyapunov function

$$V = \frac{1}{2}Li^2 \tag{19}$$

with time derivative

$$\begin{aligned}\dot{V} &= -(r+w)\,i^2 + v_s i \\ &\le -(r+w_{min})\,i^2 + v_s i < 0,\ \forall\,|i| > \frac{|v_s|}{r+w_{min}}\end{aligned} \tag{20}$$

which proves that system (17) is input-to-state stable (ISS) [43] and since the grid voltage is assumed to have a constant amplitude (stiff grid), then the inductor current will be bounded for all $t \ge 0$. Then, the remaining dynamics (18) can be written as

$$\frac{1}{2}C\frac{dV_{dc}^2}{dt} = -\frac{V_{dc}^2}{R_L} + wi^2 \tag{21}$$

which is a first-order differential equation of V_{dc}^2 with input wi^2. This system is bounded-input bounded-state stable and since w and i are proven to remain bounded, then V_{dc}^2 is bounded and consequently V_{dc} is bounded. Therefore, the closed-loop system solution $\begin{bmatrix} i(t) & V_{dc}(t) & w(t) & w_q(t)\end{bmatrix}^T$ will remain bounded for all $t \ge 0$.

Although the boundedness of the closed-loop system is proven by considering a single load resistor R_L, it also holds true for any strictly dissipative load connected at the output of the rectifier with input V_{dc} and output the load current i_L, suitably extending the proposed controller application to rectifiers with more complicated loads (e.g. nonlinear, power converter-fed loads [7]). Taking into account the parasitic elements of the converter, the proof directly follows since for a strictly dissipative load there exists $V_l(q) \ge 0$ and $\psi(q) > 0$, such that $\dot{V}_l \le V_{dc}i_L - \psi(q)$, where $q = \begin{bmatrix} i_L & q_1 & \dots & q_{n-1}\end{bmatrix}^T \in R^n$ is the load state vector [43].

As a result, a maximum bound for the rectifier and load states can be always guaranteed with the proposed strategy. However, in practice a very important issue for the rectifier operation is to guarantee a given limit for the input current below a certain value. Since i is an ac signal, it is required for its RMS value I to remain below a given maximum value I_{max}. This also corresponds to a maximum allowed power of the system given as $P_{max} = V_s I_{max}$ (since unity power factor is achieved). According to (20) and taking into account that $v_s = \sqrt{2}V_s \sin\omega t$, it is proven that

$$|i| \le \frac{\sqrt{2}V_s}{r+w_{min}},\ \forall t \ge 0, \tag{22}$$

if initially $i(0)$ satisfies the above inequality, indicating that i introduces an ultimate bound, since according to the ISS property, the derivative of the Lyapunov function (19) is negative outside of this area. Inequality (22) can be expressed using the RMS value of the current as

$$I \le \frac{V_s}{r+w_{min}}, \tag{23}$$

because (22) is satisfied for all $t \ge 0$. Since it is required that $I \le I_{max}$ at all times, then the controller parameter w_{min} can be chosen as

$$w_{min} = \frac{V_s}{I_{max}} - r \approx \frac{V_s}{I_{max}}, \tag{24}$$

since the inductor resistance r is usually considered very small and can be neglected. As a result, by selecting w_{min} according to (24), then $I(t) < I_{max}$, $\forall t \ge 0$. It should be mentioned that due to the neglected parasitic resistance r and the small phase shifting of the filter inductor, the actual current will be limited to a slightly lower value than I_{max} but as it is already analytically proven, it will be $I(t) < I_{max}$, $\forall t \ge 0$. Thus, in practice, a slightly larger I_{max} can be selected to determine w_{min} in (24).

Hence, the proposed controller can achieve an inherent current-limiting property for the rectifier without additional limiters or switching the controller operation. The controller remains continuous-time and allows the investigation of stability using nonlinear systems theory.

Now assume there exists a pair $\left(w^e,\, w_q^e\right)$ for which $w^e \in [w_{min}, w_{max}]$ corresponding to $\bar{V}_{dc} = V_{dc}^{ref}$. Then the current equation becomes

$$L\frac{di}{dt} = -(r+w^e)\,i + v_s \tag{25}$$

which represents a linear resistive-inductive RL circuit with resistance $r+w^e$. For a given $w^e>0$, system (25) asymptotically converges to a unique sinusoidal solution $i(t)$, since the system has a negative pole ($-\frac{r+w^e}{L}$) and the input v_s is sinusoidal with a constant amplitude and frequency. Using the average values and the power equivalence between ac and dc sides, at the steady state there is

$$\frac{\left(\bar{V}_{dc}^e\right)^2}{R_L}=w^e\left(I^e\right)^2$$

where $\bar{V}_{dc}^e$ is the steady-state value of $\bar{V}_{dc}$ and I^e is the RMS value of the steady-state solution $i(t)$ of (25), which results in

$$\bar{V}_{dc}^e=I^e\sqrt{R_L w^e}. \tag{26}$$

Hence, the steady-state value of the average dc output voltage $\bar{V}_{dc}^e$ is unique and according to the controller dynamics can only be V_{dc}^{ref}. Since $V_{dc}(t)>0$ (rectifier operation), then the solution $V_{dc}(t)$ of the output voltage is also unique.

However, if $\frac{\left(V_{dc}^{ref}\right)^2}{R_L}>P_{max}$ where $P_{max}=V_sI_{max}$ due to the unite power factor, i.e., if V_{dc}^{ref} is chosen very large or the load R_L changes to a small value, there will not exist a feasible w^e inside the range $[w_{min},w_{max}]$ corresponding to the desired solution. In this case, w will continuously decrease (since $\dot{\theta}<0$ from $\bar{V}_{dc}-V_{dc}^{ref}<0$ and (16)) until it reaches the minimum value w_{min} and the input current will reach the maximum value I_{max}. Note that $w\to w_{min}$ corresponds to $w_q\to 0$ which leads the angular velocity $\dot{\theta}\to 0$ according to (16). This means that $\bar{V}_{dc}$ will reach a value $\bar{V}_{dc}^e\neq V_{dc}^{ref}$ for which $\frac{\left(\bar{V}_{dc}^e\right)^2}{R_L}=P_{max}$ holds true. Therefore, even if by mistake or due to unpredicted errors the reference value V_{dc}^{ref} increases above the maximum allowed value (corresponding to the maximum allowed power P_{max}), the previous analysis still applies and the closed-loop system will guarantee the current-limiting property.

The above analysis implies that there always exists $w^e\in[w_{min},w_{max}]$ at the steady state, corresponding to a unique solution $\begin{bmatrix} i(t) & V_{dc}(t) & w(t) & w_q(t)\end{bmatrix}^T$ for the closed-loop system. However, the physical limitations of the rectifier should be considered for achieving the current-limiting property. Since the rectifier represents a boost power electronic device, the dc output voltage introduces a minimum limit, which assuming sinusoidal PWM operation, results in $\sqrt{2}V_s$. By neglecting the parasitic resistance of the inductor and taking into account the power equivalence, it results in

$$P_{max} \;=\; V_sI_{max}=\frac{\bar{V}_{dc}^2}{R_L}\geq\frac{2V_s^2}{R_L},$$

which defines the allowed range of the load resistance

$$R_L\geq\frac{2V_s}{I_{max}}. \tag{27}$$

This is a limitation of the rectifier since for a smaller load resistance, the input current will increase since the current can flow through the diodes independently from the control design. By taking into consideration all of these properties, asymptotic convergence to a unique solution can be proven as shown below.

Particularly, if (27) is satisfied for the load, then the closed-loop system states are bounded and a current-limiting property $I<I_{max}$ is achieved. As explained in the previous analysis, in this case there exists $w^e\in[w_{min},w_{max}]$ corresponding to a unique solution of the closed-loop system. Since w and w_q operate exclusively on W_0, i.e., given from (12)-(13), then for a sufficiently small $c>0$ in the controller design, the closed-loop system can be investigated as a two time-scale system with slow dynamics (12)-(13) and fast dynamics (17)-(18) as described in [43]. The fast current and voltage dynamics (17)-(18) (with respect to the controller dynamics) are investigated using the frozen parameter w. As in the case of (25), the current dynamics asymptotically converge to a unique solution depending on the frozen parameter w. Since w is proven to remain bounded inside the given range $w\in[w_{min},w_{max}]$, then asymptotic stability of the solution $i(t,w)$ holds uniformly in w, which is sinusoidal since the system represents a typical RL circuit with positive resistance $r+w$ (see equation (25)). Consequently, the voltage dynamics (21) asymptotically converge to a solution $V_{dc}(t,w)$ uniformly in the frozen parameter w since it can be viewed as a linear system with state V_{dc}^2, input wi^2, which has a negative real pole, i.e. $-\frac{2}{CR_L}$. Then, taking into account (26), it yields

$$\bar{V}_{dc}(w)=I^e(w)\sqrt{R_Lw}. \tag{28}$$

As a result, (28) introduces the boundary layer of the system. In this way, the slow controller dynamics (12)-(13) become

$$\dot{w} \;=\; c\left(I^e(w)\sqrt{R_Lw}-V_{dc}^{ref}\right)w_q^2 \tag{29}$$

$$\dot{w}_q \;=\; -\frac{c(w-w_m)w_q}{\Delta w_{max}^2}\left(I^e(w)\sqrt{R_Lw}-V_{dc}^{ref}\right), \tag{30}$$

This represents a stable second-order autonomous system in the sense of boundedness which, according to the analysis presented in Subsection III-A, cannot have a periodic solution on the ellipse of W_0. Additionally, no chaotic solution exists for (29)-(30) based on the Poincare-Bendixon theorem [46] and as a result the controller states w and w_q will asymptotically converge to one of the equilibrium points: i) $\left(w^e,w_q^e\right)$ corresponding to $\bar{V}_{dc}^e=I^e(w^e)\sqrt{R_Lw^e}=V_{dc}^{ref}$, ii) $(w_{min},0)$, or iii) $(w_{max},0)$, since they represent the possible positive limit points of system (29)-(30) inside the bounded range depending on the value of V_{dc}^{ref} [43, Lemma 4.1]. As a result, for a sufficiently small $c>0$, the nonlinear closed-loop system (17)-(18), (4)-(5) asymptotically converges to a unique solution $\begin{bmatrix} i(t) & V_{dc}(t) & w^e & w_q^e\end{bmatrix}^T$, satisfying the current-limiting property $I<I_{max}$ [43]. As previously explained, the steady-state value $\bar{V}_{dc}^e$ satisfies $\bar{V}_{dc}^e=V_{dc}^{ref}$ when $\frac{\left(V_{dc}^{ref}\right)^2}{R_L}\leq P_{max}$ or $\bar{V}_{dc}^e=\sqrt{V_sI_{max}R_L}<V_{dc}^{ref}$ when $\frac{\left(V_{dc}^{ref}\right)^2}{R_L}>P_{max}$.

Since the controller parameter c should not be chosen very high, an analytic framework for defining its value along with the rest of the controller parameters is required to be obtained. This is described in the following subsection.

C. Controller parameters selection

Having defined w_{min} from (24), the rest of the controller parameters should be also suitably designed as follows:

Parameter k: As it has been seen from (5), the parameter k is multiplied by the term $\frac{(w-w_m)^2}{\Delta w_m^2}+w_q^2-1$, which is zero on the ellipse W_0. Hence, the role of k is to make the controller dynamics of w_q robust with respect to external disturbances or calculation errors since if w and w_q are disturbed from W_0 for any reason, they will quickly return to their initial trajectory. Therefore, k should be chosen sufficiently large in order for the controller states w and w_q to be quickly attracted and stay on the desired ellipse.

Parameters w_m and Δw_m: The ellipse W_0 defines the maximum and minimum value of w which are $w_{max}=w_m+\Delta w_m$ and $w_{min}=w_m-\Delta w_m$, respectively. Parameter w_{min} is chosen from (24) for a given maximum value I_{max} of the current. In the same framework, w_{max} corresponds to a minimum input current value I_{min} from the expression

$$w_{max}\approx\frac{V_s}{I_{min}} \tag{31}$$

since the RMS value of v is approximately equal to the RMS value of the grid voltage V_s, due to the negligible voltage drop on the inductor. For a given constant load R_L, there exists a minimum current I_{min} since the rectifier represents a boost power electronic device with $\bar{V}_{dc}\geq\sqrt{2}V_s$ (for sinusoidal PWM). Therefore, I_{min} can be calculated as

$$I_{min}=\frac{2V_s}{R_L}. \tag{32}$$

However, (32) depends on the load R_L and if the load changes, the current might reach lower values. In practice, the controller should be able to operate for any load and even in the case of no load connected to the output. Since in the case of no load, a small current of mA or μA still flows through the converter due to the parasitic elements of the system, i.e. the inductor, the capacitor and the switches, I_{min} can be chosen relatively small to cover all load cases. It should be noted that in a common control operation of a rectifier, when the current drops to very small values, the PWM is turned OFF and the converter operates as a diode rectifier since there is practically no current measured to define the power factor. Therefore, parameter w_{max} is calculated from (31) for a relatively small current I_{min}.

Now, taking into account (24) and (31), the controller parameters w and Δw_m are obtained as

$$w_m = \frac{w_{max}+w_{min}}{2}=\frac{V_s}{2}\left(\frac{1}{I_{min}}+\frac{1}{I_{max}}\right), \tag{33}$$

$$\Delta w_m = \frac{w_{max}-w_{min}}{2}=\frac{V_s}{2}\left(\frac{1}{I_{min}}-\frac{1}{I_{max}}\right). \tag{34}$$

Parameter c: To define a framework for choosing the value of c, a worst case scenario is considered where w starts from w_{max} and reaches the minimum value w_{min} at the steady state, by operating on the upper semi-ellipse of W_0. In this case, the system starts from a minimum output voltage $V_{dc}^{initial}$ and reaches a maximum voltage $\bar{V}_{dc}^{e}=\sqrt{V_sI_{max}R_L}$ (depending on I_{max}), i.e. there is a maximum difference $\Delta V_{dc}^{max}=\left|V_{dc}^{initial}-\bar{V}_{dc}^{e}\right|$. If one assumes that t_s is the settling time needed for w and w_q to travel the whole upper semi-ellipse of W_0, which corresponds to an arc with central angle of πrad, with an angular velocity $\dot{\theta}$, then in the worst case the angular velocity will be $\frac{\pi}{t_s}rad/sec$ (if assumed constant and equal to its maximum value). On this trajectory, the second controller state w_q is always less or equal to 1. Then, one can define the maximum angular velocity $\dot{\theta}_{max}$ (where $w_q=1$ and $\left|\bar{V}_{dc}-V_{dc}^{ref}\right|=\Delta V_{dc}^{max}$) to be equal to $\frac{\pi}{t_s}rad/sec$ as

$$\dot{\theta}_{max}=\frac{c\Delta V_{dc}^{max}}{\Delta w_m}=\frac{\pi}{t_s}. \tag{35}$$

Then parameter c is obtained as

$$c=\frac{\pi\Delta w_m}{t_s\Delta V_{dc}^{max}} \tag{36}$$

for a maximum difference ΔV_{dc}^{max} required and a given settling time t_s. In practice, since the angular velocity decreases as soon as $\bar{V}_{dc}$ approaches V_{dc}^{ref} and also $w_q\leq 1$, then parameter c can take larger values, or in other words the settling time t_s can be chosen much smaller than the original value. Expression (36) just provides a starting value of c for a smooth response. Then c can be increased until a satisfactory response is achieved.

After selecting the controller parameters, the proposed current-limiting controller can be implemented as shown in Fig. 3, where it is clear that no PLL or instantaneous measurement of the grid voltage is required for the implementation of the controller, opposed to the traditional techniques. This significantly simplifies the implementation of the proposed controller and increases the reliability of the system. It should be noted that a low-pass filter is added at the measurement of the output voltage V_{dc} to remove the second-order harmonics and a phase-lead low-pass filter is added at the measurement of the current i to remove the switching ripples and also apply a small phase-shifting (if needed) in order to obtain unity power factor at the whole system instead of the input of the rectifier, i.e., to cancel the small phase shifting caused by the inductor L [1].

D. Controller performance under grid voltage variations

Although it is proven that the proposed controller can limit the current when unrealistic values of V_{dc}^{ref} are applied, one of the most challenging tasks is to limit the current under variations of the grid voltage and especially under voltage dips. According to the ISS analysis, it is proven that $I<I_{max}$ when w_{min} is selected according to (24). In this case, the grid voltage is considered stiff and $V_s=V_n$, where V_n is the rated RMS voltage. If it is assumed that the grid voltage introduces variations, i.e. $V_s\in[0,V_{max}]$, where V_{max} is the maximum value of the RMS grid voltage, then following the same ISS analysis and taking into account (22)-(23), it yields that

$$I\leq\frac{V_{max}}{r+w_{min}},\,\forall t\geq 0, \tag{37}$$

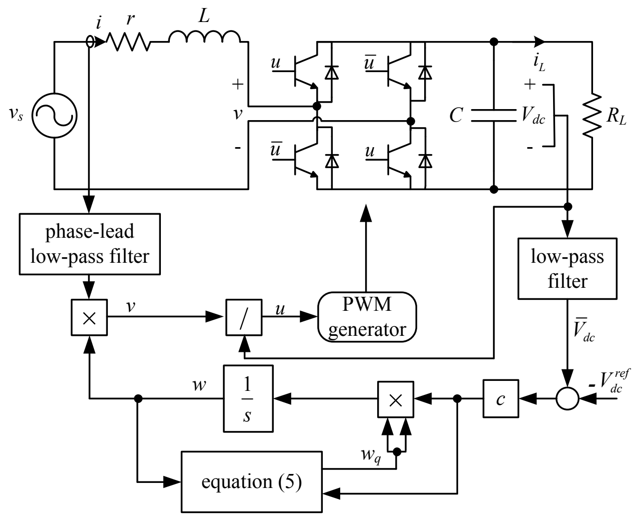

Figure 3. Implementation of the proposed current-limiting controller

as long as initially the RMS value of the current satisfies the above inequality. Hence, by selecting

$$w_{min} = \frac{V_{max}}{I_{max}} \tag{38}$$

then $I(t) < I_{max}$, $\forall t \geq 0$, which guarantees the current-limiting property even when the grid voltage varies. This includes the case where a voltage dip occurs. In order to calculate the maximum current during a voltage dip, consider the case where w_{min} is selected according to (38) and suddenly a $p \times 100\%$ percentage drop occurs at the grid voltage, where $0 \leq p \leq 1$, i.e. the RMS grid voltage becomes $(1-p)V_s$, where V_s was the original value of the grid voltage before the fault. Then according to (23) there is

$$I \leq \frac{(1-p)\,V_s}{r + \frac{V_{max}}{I_{max}}} < (1-p)\frac{V_s}{V_{max}} I_{max} < (1-p)I_{max}. \tag{39}$$

Inequality (39) implies that the current will be limited below a lower value depending on the percentage of the voltage dip. This is due to the fact that the measurement of the grid voltage is not used for the controller design, which significantly simplifies its implementation. Nevertheless, in any case, the input current will be lower than I_{max} as required to protect the rectifier. Note that the same controller can be extended to applications with an LCL filter instead of an L filter, where the capacitor voltage remains in the range $[0, V_{max}]$, depending on the grid voltage and the filter parameters.

IV. Experimental validation

In order to verify the efficiency of the proposed controller, a single-phase full-bridge rectifier with a load resistor R_L operating under the proposed current-limiting controller described in Fig. 3 was experimentally investigated. A switching frequency of 19 kHz was used for the PWM operation and the proposed controller was implemented using the TMS320F28335 DSP with a sampling frequency of 16 kHz. The system and the controller parameters are given in Table I. Because of the limitations of the input voltage level for

Table I
System and controller parameters

Parameters	Values	Parameters	Values
L	2.2 mH	I_{max}	3 A
r	0.5 Ω	I_{min}	1 mA
C	1650 μF	k	100
R_L	100 ∼ 320 Ω	t_s	0.4 s
V_s	36 V	ΔV_{dc}^{max}	50 V
ω	100π rad/s	w_0	60 Ω

the experimental setup, a 36 V RMS input voltage was used due to the popularity of 110 V/36 V transformers. For the controller implementation, the low-pass filter $\frac{1}{0.01s+1}$ was used at the measurement of the dc output voltage to reject the second-order harmonics and the phase-lead low-pass filter $\frac{31(0.06s+1)}{(0.003s+1)(s+270)}$ was used at the measurement of the inductor current to remove the switching ripples and apply a small phase shifting to cancel the effect of the filter inductor. This is commonly used in power converter control applications when a feed-forward term is introduced at the control signal [1]. Note that different types of filters can be used for both measurements (e.g. hold filter for the dc output voltage) but the above filters were considered for simplicity.

A. Operation with normal grid

Initially, the system operates as a diode rectifier with $V_s = 36$ V and $R_L = 320\,\Omega$, and the controller is not active. Fig. 4(b) shows the transient response when the controller is enabled with $V_{dc}^{ref} = 110$ V, which corresponds to a typical voltage level in ac or dc power applications. The dc output voltage increases and smoothly converges to the reference value after a short transient, while the unity power factor is maintained during the whole operation. Note that the transient response can be faster if the capacitance C is reduced, but this will increase the second-order ripples of the output voltage. The smooth transient is due to the proposed controller which applies a varying resistance starting from $w_0 = 60\,\Omega$ and reduces while moving on the desired ellipse W_0, as shown in Fig. 4(c) and 4(d). The initial condition of w_q was defined as $w_{q0} = \sqrt{1 - \frac{(w_0 - w_m)^2}{\Delta w_m^2}} = 0.073$ according to (10). Hence, the proposed strategy additionally offers a soft start-up solution of the closed-loop system. Then, the load suddenly changes from 320 Ω to 220 Ω, and the output voltage is regulated at the reference value after a short transient as shown in Fig. 5(b). The transient response of the controller states is shown in Fig. 5(c) and it is verified in Fig. 5(d) that they exclusively operate on the desired ellipse W_0. The steady-state responses of the output voltage, the grid voltage and the inductor current are shown in Fig. 5(a). It is clear that almost unity power factor is achieved (over 0.98 measured which is acceptable in practice) and the output voltage is regulated at the desired value $V_{dc}^{ref} = 110$ V with small second-order harmonics caused by the full-bridge rectifier operation. Due to the limitation of the experimental setup, although the current waveforms have been obtained from a power analyzer, the current measurement used for the controller implementation was provided from inside the power module, which reduces the

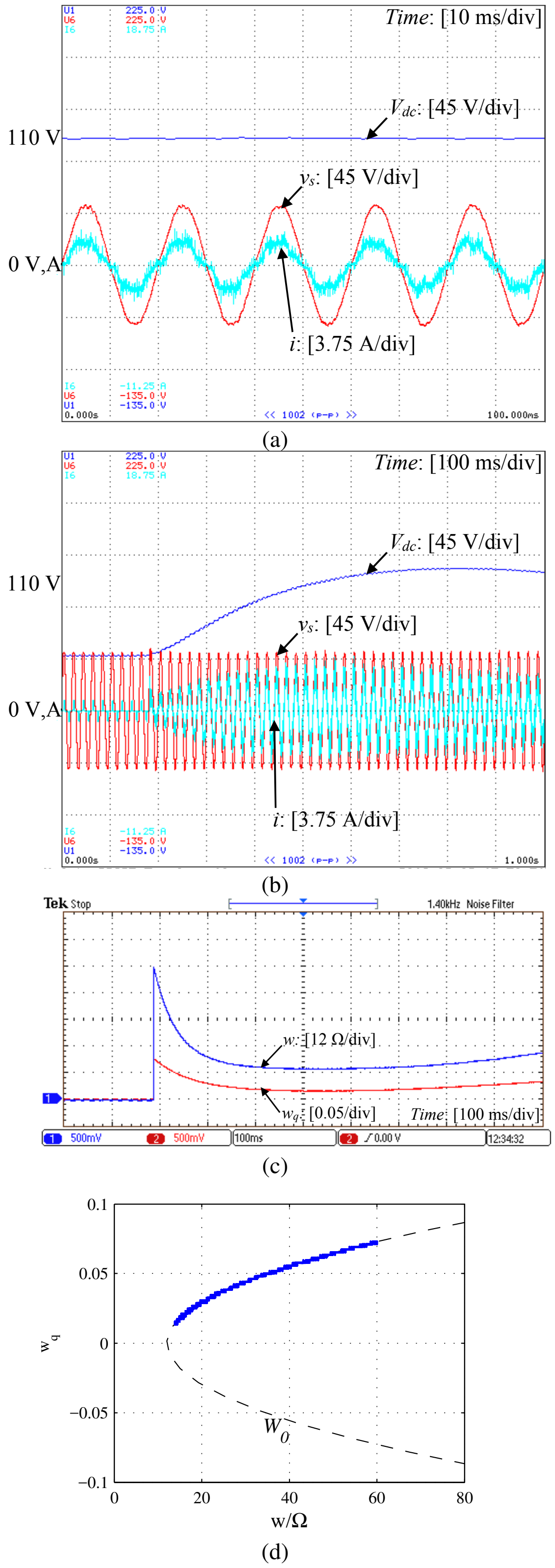

Figure 4. Experimental results of the proposed current-limiting controller under normal operation when the controller is enabled with $V_{dc}^{ref} = 110\,\mathrm{V}$ and $R_L = 320\,\Omega$: (a) steady-state response of the system states, (b) transient response of the system states, (c) transient response of the controller states, (d) $w - w_q$ plane.

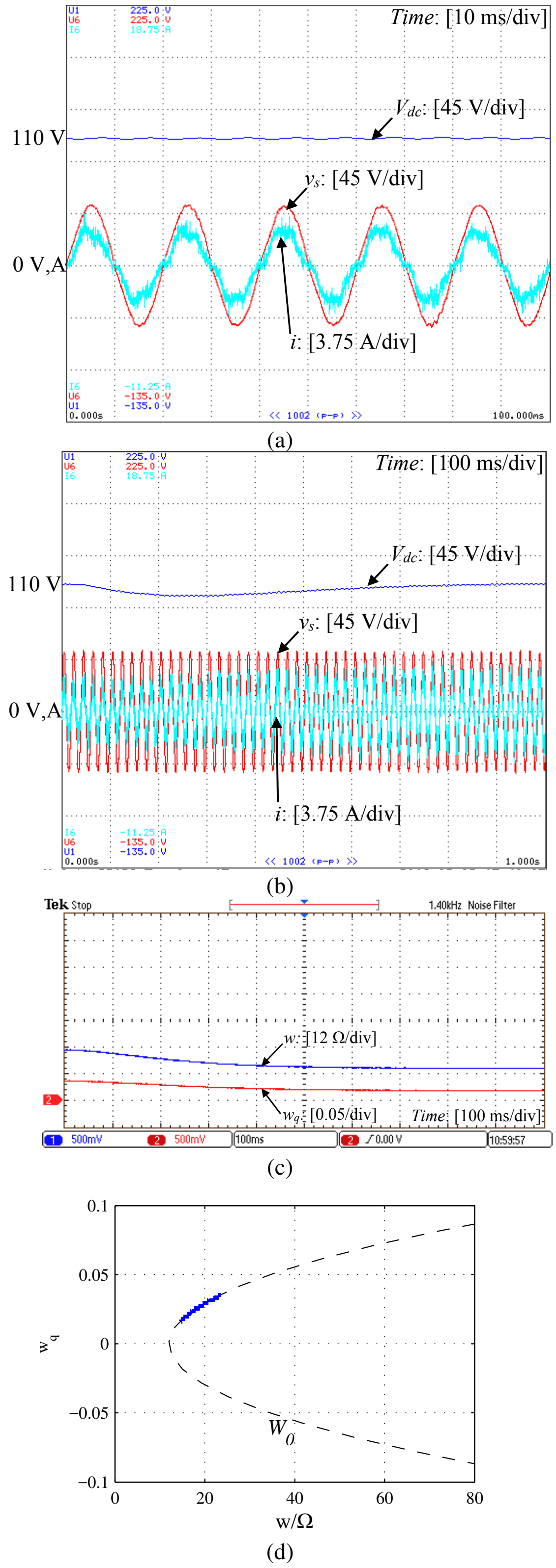

Figure 5. Experimental results of the proposed current-limiting controller under normal operation when the load changes from $320\,\Omega$ to $220\,\Omega$ with $V_{dc}^{ref} = 110\,\mathrm{V}$: (a) steady-state response of the system states, (b) transient response of the system states, (c) transient response of the controller states, (d) $w - w_q$ plane.

accuracy of the measurement and has an impact on the power quality. Note that different current measurement units, filter design or PWM techniques that improve the total harmonic distortion of the current can be applied using the proposed controller [47], [48], [49], and are currently investigated.

In order to verify the current-limiting property of the controller, the reference output voltage changes from 110 V to 140 V, when the load resistor is 220 Ω. However, as it becomes clear from Fig. 6(a), the output voltage is regulated at around 120 V because the current tries to violate the maximum limit. Although the limit of the current was set to $I_{max} = 3$ A, the RMS value of the steady-state current was measured at 2.2 A which is slightly less than I_{max}, since as mentioned in Subsection III-B w_{min} is calculated from (24) where the parasitic resistance r of the inductor L was neglected and the power factor is slightly less than 1. However, this still results in $I < I_{max}$ which is desired. In practice, I_{max} can be chosen slightly higher for the selection of w_{min} to cope with this issue. According to the transient response of the controller states (Fig. 6(c)), $w \rightarrow w_{min}$ and $w_q \rightarrow 0$ as expected at the limit of the current. This is also shown from the controller state trajectory on the ellipse W_0 on the $w - w_q$ plane, in Fig. 6(d), verifying the theory developed in the paper.

To further validate the current limitation, while the reference dc output voltage is kept constant at $V_{dc}^{ref} = 110$ V, the load changes from 320 Ω to 100 Ω, which is a larger change than the one described in Fig. 5. This causes the input current to increase and be limited again at 2.2 A. This leads to a drop of the output voltage from 110 V to 82 V, as shown from the transient and the steady-state responses of the system states in Fig. 7(b) and Fig. 7(a), respectively. Hence, the proposed controller automatically reduces the output voltage to protect the rectifier from large currents. The controller states w and w_q tend to w_{min} and 0, respectively, while operating exclusively on W_0, as shown in Fig. 7(c) and Fig. 7(d).

B. Operation under grid voltage dips

In order to further test the current-limiting capability of the proposed controller, two scenarios of voltage dips at the grid voltage are investigated. The desired output voltage is again set at 110 V and the load resistance is $R_L = 220\,\Omega$ for the whole operation. Initially, the RMS grid voltage drops from 36 V to 30 V, which corresponds to a 17% voltage drop, i.e. $p = 0.17$. According to the analysis of Subsection III-D, the current will be limited to a lower value corresponding to 83% of the maximum current. As shown in Fig. 8(b), the current increases as the voltage drops and its RMS value is limited at 1.82 A, as verified from the steady state response of Fig. 8(a). Since the experimental results of Fig. 6 have indicated that the given controller limits the current at a maximum value of 2.2 A, then the analysis of Subsection III-D proves that the current should be limited below $0.83 \times 2.2\,\text{A} = 1.83\,\text{A}$, which is the case. The output voltage drops to a lower value to maintain the power equivalence. The controller states w and w_q are regulated at their minimum values w_{min} and 0, respectively, as shown in Fig. 8(c), and their trajectory stays on W_0, as shown in Fig. 8(d).

Finally, the RMS of the grid voltage suddenly drops from 36 V to 23 V (36% voltage drop) and the results are shown in Fig. 9. The transient response is illustrated in Fig. 9(b) where the output voltage drops and is regulated to a value lower than the reference (around 77 V) because the input current is limited at 1.38 A, as expected from the theory ($0.64 \times 2.2\,\text{A} = 1.4\,\text{A}$).

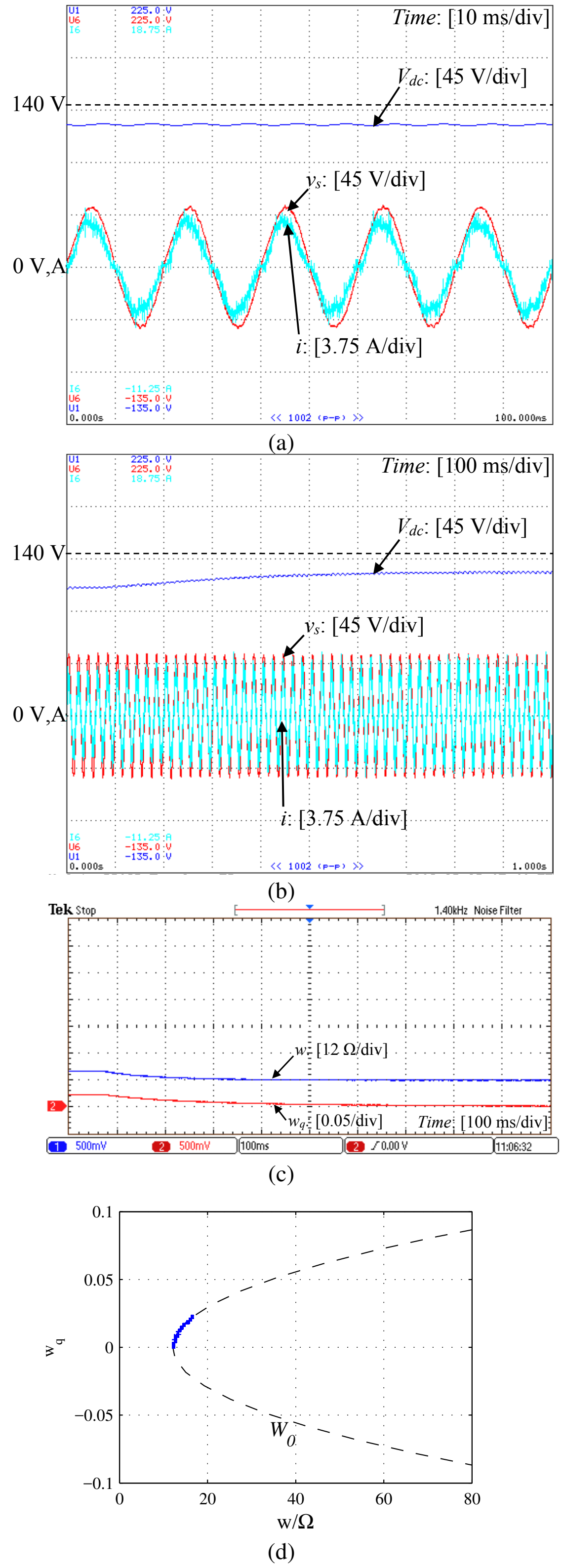

Figure 6. Experimental results of the proposed controller reaching the current limit when the V_{dc}^{ref} changes from 110 V to 140 V (current limiting activated with $\bar{V}_{dc} \rightarrow 120$ V): (a) steady-state response of the system states, (b) transient response of the system states, (c) transient response of the controller states, (d) $w - w_q$ plane.

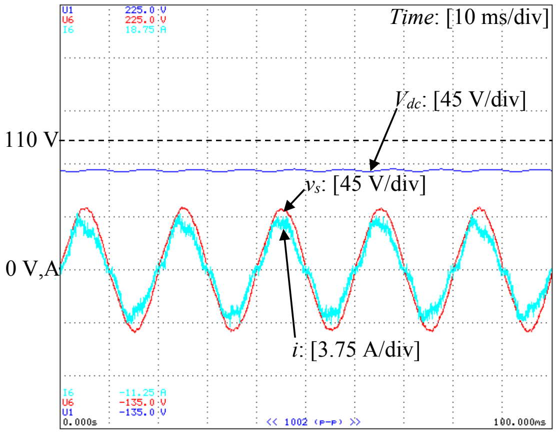

(a)

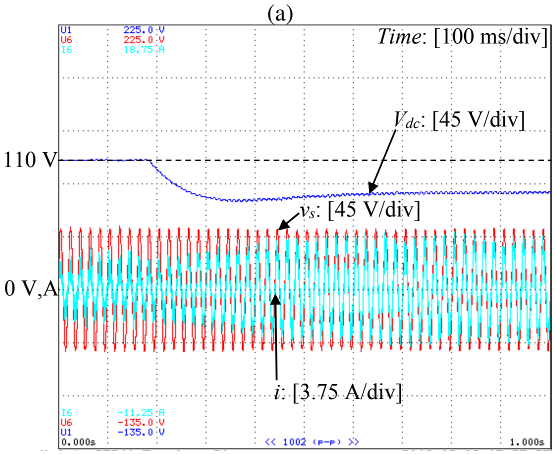

(b)

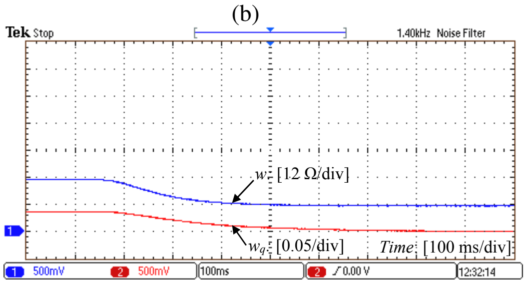

(c)

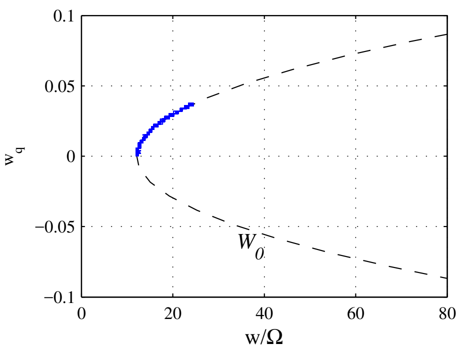

(d)

Figure 7. Experimental results of the proposed controller reaching the current limit when the load changes from 320 Ω to 100 Ω with $V_{dc}^{ref} = 110$ V (current limiting activated with $\bar{V}_{dc} \to 82$ V): (a) steady-state response of the system states, (b) transient response of the system states, (c) transient response of the controller states, (d) $w - w_q$ plane.

This is clearly shown from the steady-state response of Fig. 9(a). As in the previous case, the controller states w and w_q converge to w_{min} and 0, respectively, while moving on the desired ellipse (Fig. 9(c) and Fig. 9(d)). As a result, it is verified that even when voltage dips occur at the grid, the proposed controller maintains the input current below a maximum value without requiring the measurement of the grid voltage, sag detection mechanisms or additional protection devices.

V. Conclusions

In this paper, a nonlinear controller with an inherent current-limiting capability was proposed for single-phase rectifiers. The developed strategy guarantees nonlinear asymptotic stability and convergence to a unique solution at all times, while achieving the main tasks of the rectifier operation, i.e., accurate output voltage regulation and unity power factor operation. An analytic description of the controller parameters selection was provided to guarantee that the input current will be limited below a given value during transients even if the grid voltage varies. Opposed to the existing control techniques, the proposed current-limiting controller is fully independent from the system parameters and does not require a PLL or the instantaneous measurement of the grid voltage, leading to a simplified implementation. Extensive experimental results were provided to support the theoretical background of the proposed approach and verify its effective operation.

It is worth noting that the use of a positive dynamic virtual resistance in the proposed controller structure can guarantee the required stability but restricts the proposed controller application only to rectifiers and not to inverters. Hence, this represents a simplified control approach for rectifier-fed passive loads. Further investigation is required to obtain a generic structure that can be applied to both types of ac/dc converters with different operating conditions (e.g. constant power, constant current loads) and satisfy some additional practical limitations (e.g. saturation of the control input) with an improvement of the power quality. These issues represent interesting topics for future research.

References

[1] Q.-C. Zhong and T. Hornik, *Control of Power Inverters in Renewable Energy and Smart Grid Integration.* Wiley-IEEE Press, 2013.

[2] C. Meza, D. Biel, D. Jeltsema, and J. M. A. Scherpen, "Lyapunov-Based Control Scheme for Single-Phase Grid-Connected PV Central Inverters," *IEEE Trans. Control Syst. Technol.*, vol. 20, no. 2, pp. 520–529, 2012.

[3] G. C. Konstantopoulos and Q.-C. Zhong, "Current-limiting non-linear controller for single-phase AC/DC PWM power converters," in *2015 American Control Conference (ACC)*, Chicago, IL, July 1-3 2015, pp. 1029–1034.

[4] J. G. Hwang, P. W. Lehn, and M. Winkelnkemper, "A generalized class of stationary frame-current controllers for grid-connected AC-DC converters," *IEEE Trans. Power Del.*, vol. 25, no. 4, pp. 2742–2751, Oct 2010.

[5] O. Stihi and B.-T. Ooi, "A single-phase controlled-current PWM rectifier," *IEEE Trans. Power Electron.*, vol. 3, no. 4, pp. 453–459, 1988.

[6] O. Kükrer and H. Kömürcügil, "Control strategy for single-phase PWM rectifiers," *Electronics Letters*, vol. 33, no. 21, pp. 1745–1746, 1997.

[7] D. Karagiannis, E. Mendes, A. Astolfi, and R. Ortega, "An experimental comparison of several PWM controllers for a single-phase AC-DC converter," *IEEE Trans. Control Syst. Technol.*, vol. 11, no. 6, pp. 940–947, 2003.

[8] W. Song, Z. Deng, S. Wang, and X. Feng, "A simple model predictive power control strategy for single-phase PWM converters with modulation function optimization," *IEEE Trans. Power Electron.*, vol. 31, no. 7, pp. 5279 – 5289, 2016.

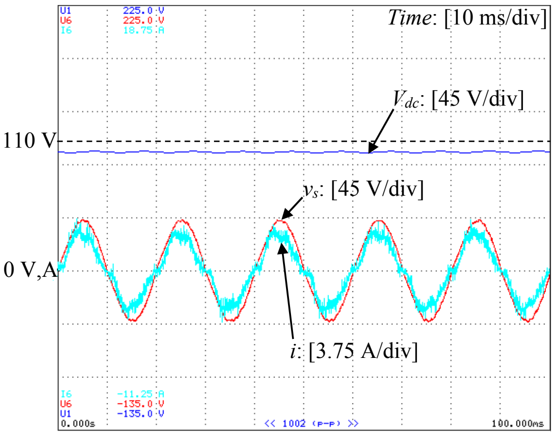

(a)

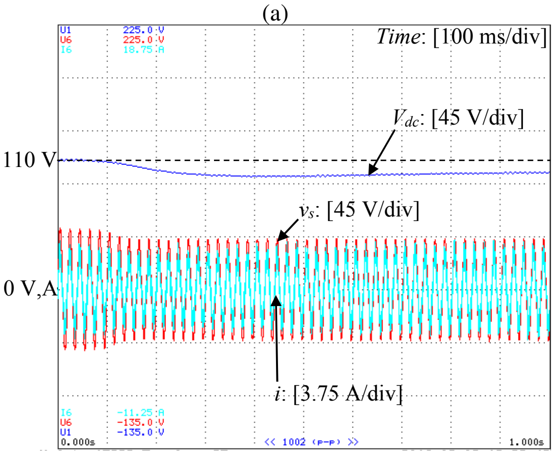

(b)

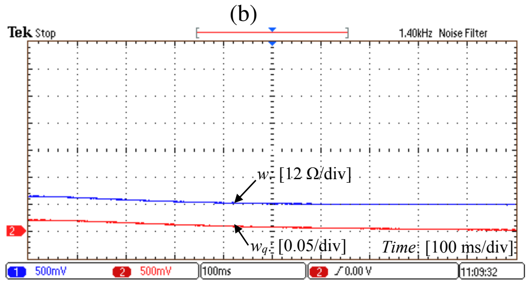

(c)

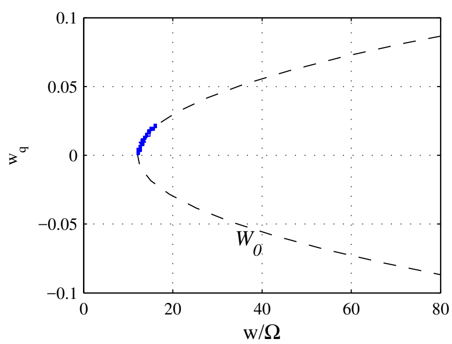

(d)

Figure 8. Experimental results of the proposed current-limiting controller when the RMS input voltage changes from 36 V to 30 V (current limiting activated with $\bar{V}_{dc} \to 100$ V): (a) steady-state response of the system states, (b) transient response of the system states, (c) transient response of the controller states, (d) $w - w_q$ plane.

[9] T.-S. Lee, “Lagrangian modeling and passivity-based control of three-phase AC/DC voltage-source converters,” *IEEE Transactions on Industrial Electronics*, vol. 51, no. 4, pp. 892–902, 2004.

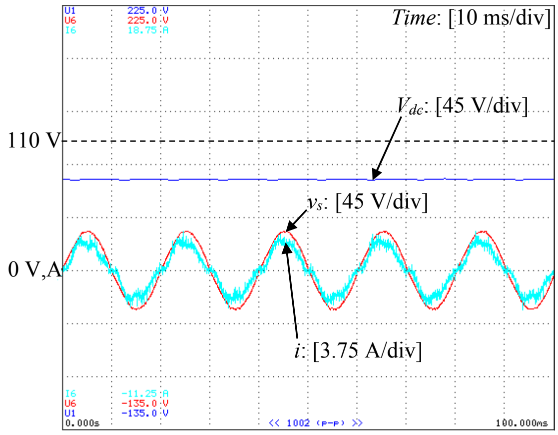

(a)

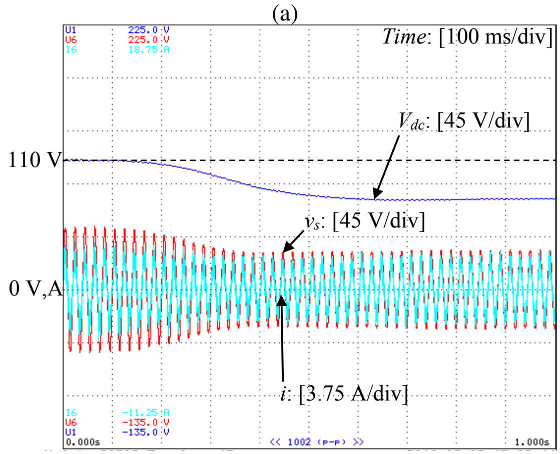

(b)

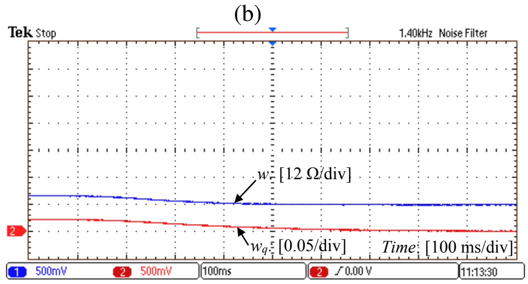

(c)

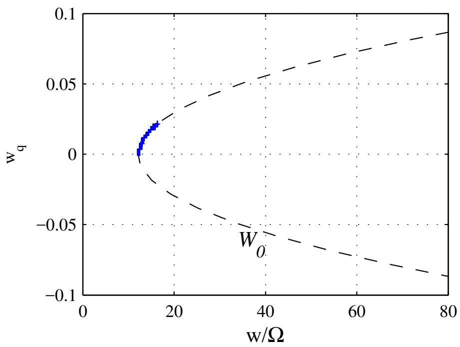

(d)

Figure 9. Experimental results of the proposed current-limiting controller when the RMS input voltage changes from 36 V to 23 V (current limiting activated with $\bar{V}_{dc} \to 77$ V): (a) steady-state response of the system states, (b) transient response of the system states, (c) transient response of the controller states, (d) $w - w_q$ plane.

[10] F. Giri, A. Abouloifa, I. Lachkar, and F. Zahra Chaoui, “Formal framework for nonlinear control of PWM AC/DC coost rectifiers—controller design and average performance analysis,” *IEEE Trans. Control Syst.*

Technol., vol. 18, no. 2, pp. 323–335, 2010.
[11] T. Jin, L. Li, and K. M. Smedley, "A universal vector controller for four-quadrant three-phase power converters," *IEEE Trans. Circuits Syst. I: Reg. Papers*, vol. 54, no. 2, pp. 377–390, 2007.
[12] D. del Puerto-Flores, J. M. A. Scherpen, M. Liserre, M. M. J. de Vries, M. J. Kransse, and V. Giuseppe Monopoli, "Passivity-based control by series/parallel damping of single-phase PWM voltage source converter," *IEEE Trans. Control Syst. Technol.*, vol. 22, no. 4, pp. 1310–1322, 2014.
[13] T.-S. Lee, "Input-output linearization and zero-dynamics control of three-phase AC/DC voltage-source converters," *IEEE Trans. Power Electron.*, vol. 18, no. 1, pp. 11–22, 2003.
[14] H. Kömürcügil and O. Kükrer, "Lyapunov-based control for three-phase PWM AC/DC voltage-source converters," *IEEE Trans. Power Electron.*, vol. 13, no. 5, pp. 801–813, 1998.
[15] A. Gensior, H. Sira-RamÃ■rez, J. Rudolph, and H. GÃijldner, "On some nonlinear current controllers for three-phase boost rectifiers," *IEEE Trans. Industrial Electron.*, vol. 56, no. 2, pp. 360–370, 2009.
[16] Y. Zhang, Y. Peng, and H. Yang, "Performance improvement of two-vectors-based model predictive control of PWM rectifier," *IEEE Trans. Power Electron.*, vol. 31, no. 8, pp. 6016 – 6030, 2016.
[17] O. Kukrer, H. Komurcugil, and A. Doganalp, "A three-level hysteresis function approach to the sliding-mode control of single-phase UPS inverters," *IEEE Trans. Ind. Electron.*, vol. 56, no. 9, pp. 3477–3486, 2009.
[18] A. Dell' Aquila, M. Liserre, V. Giuseppe Monopoli, and P. Rotondo, "Overview of PI-based solutions for the control of DC buses of a single-phase H-bridge multilevel active rectifier," *IEEE Trans. Ind. Appl.*, vol. 44, no. 3, pp. 857–866, 2008.
[19] R. Teodorescu, F. Blaabjerg, M. Liserre, and P. C. Loh, "Proportional-resonant controllers and filters for grid-connected voltage-source converters," *IEE Proc.-Electric Power Applications*, vol. 153, no. 5, pp. 750–762, 2006.
[20] C. Cecati, A. Dell'Aquila, M. Liserre, and A. Ometto, "A fuzzy-logic-based controller for active rectifier," *IEEE Trans. Ind. Appl.*, vol. 39, no. 1, pp. 105–112, Jan 2003.
[21] R. Ghosh and G. Narayanan, "A single-phase boost rectifier system for wide range of load variations," *IEEE Trans. Power Electron.*, vol. 22, no. 2, pp. 470–479, 2007.
[22] R. Martinez and P. N. Enjeti, "A high-performance single-phase rectifier with input power factor correction," *IEEE Trans. Power Electron.*, vol. 11, no. 2, pp. 311–317, 1996.
[23] R. Ortega, A. Loria, P. J. Nicklasson, and H. Sira-Ramirez, *Passivity-based Control of Euler-Lagrange Systems, Mechanical, Electrical and Electromechanical Applications*. Springer-Verlag. Great Britain, 1998.
[24] H. Komurcugil, N. Altin, S. Ozdemir, and I. Sefa, "An extended Lyapunov-function-based control strategy for single-phase UPS inverters," *IEEE Trans. on Power Electron.*, vol. 30, no. 7, pp. 3976–3983, 2015.
[25] M. Hernandez-Gomez, R. Ortega, F. Lamnabhi-Lagarrigue, and G. Escobar, "Adaptive PI stabilization of switched power converters," *IEEE Trans. Control Syst. Technol.*, vol. 18, no. 3, pp. 688–698, 2010.
[26] G. Escobar, D. Chevreau, R. Ortega, and E. Mendes, "An adaptive passivity-based controller for a unity power factor rectifier," *IEEE Trans. Control Syst. Technol.*, vol. 9, no. 4, pp. 637–644, 2001.
[27] G. F. Montgomery, "Current-limited rectifiers," *Proceedings of the IRE*, vol. 50, no. 2, pp. 190–193, Feb 1962.
[28] C. C. Herskind and H. L. Kellogg, "Rectifier fault currents," *Electrical Engineering*, vol. 64, no. 3, pp. 145–150, March 1945.
[29] J. Lira, N. Visairo, C. Nunez, A. Ramirez, and H. Sira-Ramirez, "A robust nonlinear control scheme for a sag compensator active multilevel rectifier without sag detection algorithm," *IEEE Trans. Power Electron.*, vol. 27, no. 8, pp. 3576–3583, 2012.
[30] N. Visairo, C. Nunez, J. Lira, and I. Lazaro, "Avoiding a voltage sag detection stage for a single-phase multilevel rectifier by using control theory considering physical limitations of the system," *IEEE Trans. Power Electron.*, vol. 28, no. 11, pp. 5244–5251, 2013.
[31] P. Rioual, H. Pouliquen, and J. P. Louis, "Regulation of a PWM rectifier in the unbalanced network state using a generalized model," *IEEE Trans. Power Electron.*, vol. 11, no. 3, pp. 495–502, May 1996.
[32] A. D. Paquette and D. M. Divan, "Virtual impedance current limiting for inverters in microgrids with synchronous generators," *IEEE Trans. Ind. Appl.*, vol. 51, no. 2, pp. 1630–1638, 2015.
[33] M. Huang, S.-C. Wong, C. K. Tse, and X. Ruan, "Catastrophic bifurcation in three-phase voltage-source converters," *IEEE Trans. Circuits Syst. I: Reg. Papers*, vol. 60, no. 4, pp. 1062–1071, 2013.
[34] H. J. Laaksonen, "Protection principles for future microgrids," *IEEE Trans. Power Electron.*, vol. 25, no. 12, pp. 2910–2918, 2010.
[35] Y. Yang, F. Blaabjerg, and H. Wang, "Low-voltage ride-through of single-phase transformerless photovoltaic inverters," *IEEE Trans. Ind. Appl.*, vol. 50, no. 3, pp. 1942–1952, 2014.
[36] M. S. El Moursi, W. Xiao, and J. L. Kirtley, "Fault ride through capability for grid interfacing large scale PV power plants," *IET Generation, Transmission & Distribution*, vol. 7, no. 9, pp. 1027–1036, 2013.
[37] A. B. Youssef, S. K. E. Khil, and I. Slama-Belkhodja, "State observer-based sensor fault detection and isolation, and fault tolerant control of a single-phase PWM rectifier for electric railway traction," *IEEE Trans. Power Electron.*, vol. 28, no. 12, pp. 5842–5853, 2013.
[38] N. Bottrell and T. C. Green, "Comparison of current-limiting strategies during fault ride-through of inverters to prevent latch-up and wind-up," *IEEE Trans. Power Electron.*, vol. 29, no. 7, pp. 3786–3797, 2014.
[39] J. Rohten, J. Espinoza, J. Munoz, M. Perez, P. Melin, J. Silva, E. Espinosa, and M. Rivera, "Model predictive control for power converters in a distorted three-phase power supply," *IEEE Trans. Ind. Electron.*, to appear.
[40] L. Zaccarian and A. R. Teel, "Nonlinear scheduled anti-windup design for linear systems," *IEEE Trans. Autom. Control*, vol. 49, no. 11, pp. 2055–2061, 2004.
[41] S. Galeani, S. Onori, and L. Zaccarian, "Nonlinear scheduled control for linear systems subject to saturation with application to anti-windup control," in *46th IEEE Conference on Decision and Control*, 2007, pp. 1168–1173.
[42] S. Tarbouriech and M. Turner, "Anti-windup design: an overview of some recent advances and open problems," *IET Control Theory & Applications*, vol. 3, no. 1, pp. 1–19, 2009.
[43] H. K. Khalil, *Nonlinear Systems*. Prentice Hall, 2001.
[44] R. Sira-Ramirez, H.and Silva-Ortigoza, *Control Design Techniques in Power Electronics Devices*. Springer, London, 2006.
[45] S. Wang, X. Ruan, K. Yao, S.-C. Tan, Y. Yang, and Z. Ye, "A flicker-free electrolytic capacitor-less AC–DC LED driver," *IEEE Trans. Power Electron.*, vol. 27, no. 11, pp. 4540–4548, 2012.
[46] S. Wiggins, *Introduction to Applied Nonlinear Dynamical Systems and Chaos*, 2nd ed., N. Y. Springer, Ed., 2003.
[47] A. Kwasinski, P. T. Krein, and P. L. Chapman, "Time domain comparison of pulse-width modulation schemes," *IEEE Power Electronics Letters*, vol. 1, no. 3, pp. 64–68, 2003.
[48] S. R. Bowes and S. Grewal, "Modulation strategy for single phase pwm inverters," *Electronics Letters*, vol. 34, no. 5, pp. 420–422, 1998.
[49] M. Meco-Gutierrez, J. R. Heredia-Larrubia, F. Perez-Hidalgo, A. Ruiz-Gonzalez, and F. Vargas-Merino, "Pulse width modulation technique parameter selection with harmonic injection and frequencymodulated triangular carrier," *IET Power Electronics*, vol. 6, no. 5, pp. 954–962, 2013.

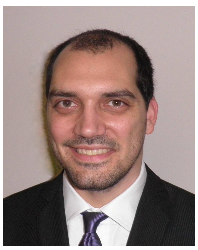

George C. Konstantopoulos (S'07-M'13) received his Diploma and Ph.D. degrees in electrical and computer engineering from the Department of Electrical and Computer Engineering, University of Patras, Rion, Greece, in 2008 and 2012, respectively.

From 2011 to 2012, he was an Electrical Engineer with the Public Power Corporation of Greece. Since 2013, he has been with the Department of Automatic Control and Systems Engineering, The University of Sheffield, U.K., where he is currently a Lecturer. His research interests include nonlinear modeling, control and stability analysis of power converters in microgrid and smart grid applications, renewable energy systems and electrical drives. Dr. Konstantopoulos is a Member of the National Technical Chamber of Greece.

Qing-Chang Zhong (M'03-SM'04) received the Ph.D. degree in control and power engineering (awarded the Best Doctoral Thesis Prize) from Imperial College London, London, U.K., in 2004 and the Ph.D. degree in control theory and engineering from Shanghai Jiao Tong University, Shanghai, China, in 2000.

He holds the Max McGraw Endowed Chair Professor in Energy and Power Engineering at the Dept. of Electrical and Computer Engineering, Illinois Institute of Technology, Chicago, USA, and the Research Professor in Control of Power Systems at the Department of Automatic Control and Systems Engineering, The University of Sheffield, UK. He is a Distinguished Lecturer of both the IEEE Power Electronics Society and the IEEE Control Systems Society. He (co-)authored three research monographs: Control of Power Inverters in Renewable Energy and Smart Grid Integration (Wiley-IEEE Press, 2013), Robust Control of Time-Delay Systems (Springer-Verlag, 2006), Control of Integral Processes with Dead Time (Springer-Verlag, 2010), and a fourth, Power Electronics-enabled Autonomous Power Systems: Next Generation Smart Grids, is scheduled for publication by Wiley-IEEE Press. He proposed the architecture for the next-generation smart grids, which adopts the synchronization mechanism of synchronous machines to unify the interface and interaction of power system players with the grid and achieve autonomous operation of power systems. His research focuses on power electronics, advanced control theory and the integration of both, together with applications in renewable energy, smart grid integration, electric drives and electric vehicles, aircraft power systems, high-speed trains etc.

He is a Fellow of the Institution of Engineering and Technology (IET), a Senior Member of IEEE, the Vice-Chair of IFAC TC of Power and Energy Systems and was a Senior Research Fellow of the Royal Academy of Engineering/Leverhulme Trust, UK (2009-2010) and the UK Representative to the European Control Association (2013-2015). He serves as an Associate Editor for IEEE Trans. on Automatic Control, IEEE Trans. on Power Electronics, IEEE Trans. on Industrial Electronics, IEEE Trans. on Control Systems Technology, IEEE Access, IEEE Journal of Emerging and Selected Topics in Power Electronics, European Journal of Control and the Conference Editorial Board of the IEEE Control Systems Society.